

Understanding and Managing Capacity Walkdown in Nickel-Hydrogen Cells and Batteries

31 May 2002

Prepared by

L. H. THALLER, A. H. ZIMMERMAN, and G. A. TO
Electronic and Photonic Laboratory
Laboratory Operations

Prepared for

SPACE AND MISSILE SYSTEMS CENTER
AIR FORCE SPACE COMMAND
2430 E. El Segundo Boulevard
Los Angeles Air Force Base, CA 90245

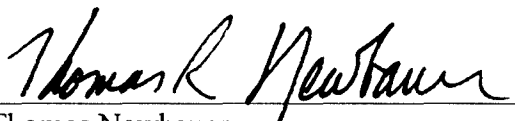
National Systems Group

APPROVED FOR PUBLIC RELEASE;
DISTRIBUTION UNLIMITED

This report was submitted by The Aerospace Corporation, El Segundo, CA 90245-4691, under Contract No. F04701-00-C-0009 with the Space and Missile Systems Center, 2430 E. El Segundo Blvd., Los Angeles Air Force Base, CA 90245. It was reviewed and approved for The Aerospace Corporation by B. Jaduszliwer, Principal Director, Electronics and Photonics Laboratory; and Glenn A. Davis, Principal Director, Space Systems, National Systems Group. Thomas Newbauer was the project officer for the program.

This report has been reviewed by the Public Affairs Office (PAS) and is releasable to the National Technical Information Service (NTIS). At NTIS, it will be available to the general public, including foreign nationals.

This technical report has been reviewed and is approved for publication. Publication of this report does not constitute Air Force approval of the report's findings or conclusions. It is published only for the exchange and stimulation of ideas.

A handwritten signature in black ink, reading "Thomas R. Newbauer". The signature is written in a cursive style with a horizontal line underneath the name.

Thomas Newbauer
SMC/AXEN

REPORT DOCUMENTATION PAGE				Form Approved OMB No. 0704-0188	
Public reporting burden for this collection of information is estimated to average 1 hour per response, including the time for reviewing instructions, searching existing data sources, gathering and maintaining the data needed, and completing and reviewing this collection of information. Send comments regarding this burden estimate or any other aspect of this collection of information, including suggestions for reducing this burden to Department of Defense, Washington Headquarters Services, Directorate for Information Operations and Reports (0704-0188), 1215 Jefferson Davis Highway, Suite 1204, Arlington, VA 22202-4302. Respondents should be aware that notwithstanding any other provision of law, no person shall be subject to any penalty for failing to comply with a collection of information if it does not display a currently valid OMB control number. PLEASE DO NOT RETURN YOUR FORM TO THE ABOVE ADDRESS.					
1. REPORT DATE (DD-MM-YYYY) 31-05-2002		2. REPORT TYPE		3. DATES COVERED (From - To)	
4. TITLE AND SUBTITLE Understanding and Managing Capacity Walkdown in Nickel-Hydrogen Cells and Batteries				5a. CONTRACT NUMBER F04701-00-C-0009	
				5b. GRANT NUMBER	
				5c. PROGRAM ELEMENT NUMBER	
6. AUTHOR(S) L. H. Thaller, A. H. Zimmerman, and G. A., To				5d. PROJECT NUMBER	
				5e. TASK NUMBER	
				5f. WORK UNIT NUMBER	
7. PERFORMING ORGANIZATION NAME(S) AND ADDRESS(ES) The Aerospace Corporation Laboratory Operations El Segundo, CA 90245-4691				8. PERFORMING ORGANIZATION REPORT NUMBER TR-2002(3000)-2	
9. SPONSORING / MONITORING AGENCY NAME(S) AND ADDRESS(ES) Space and Missile Systems Center Air Force Space Command 2450 E. El Segundo Blvd. Los Angeles Air Force Base, CA 90245				10. SPONSOR/MONITOR'S ACRONYM(S) SMC	
				11. SPONSOR/MONITOR'S REPORT NUMBER(S) SMC-TR-02-32	
12. DISTRIBUTION/AVAILABILITY STATEMENT Approved for public release; distribution unlimited.					
13. SUPPLEMENTARY NOTES					
14. ABSTRACT In this report, the findings of a recent study that investigated the impact of cycling temperature, electrolyte concentration, cobalt content of the active material, and the cycling history of the electrode on the charging potential for the beta-phase and gamma-phase materials have been incorporated into our earlier studies of the capacity walkdown phenomenon. Significant amounts of capacity walkdown were found to be associated with many of the life cycle testing programs carried out at the Navy facility in Crane, IN. These findings are not only helpful for understanding the mechanisms associated with capacity walkdown, but will be useful in selecting cell design factors and cycling conditions that will allow the capacity loss to be held to an acceptable value.					
15. SUBJECT TERMS Nickel-hydrogen cells, Capacity walkdown, Capacity maintenance					
16. SECURITY CLASSIFICATION OF:			17. LIMITATION OF ABSTRACT	18. NUMBER OF PAGES	19a. NAME OF RESPONSIBLE PERSON Larry Thaller
a. REPORT UNCLASSIFIED	b. ABSTRACT UNCLASSIFIED	c. THIS PAGE UNCLASSIFIED			19b. TELEPHONE NUMBER (include area code) (310)336-5180

Acknowledgments

The cycling data used in this report was made available from the life tests sponsored by the Air Force and NASA. The tests themselves were carried out at the Navy facility located at Crane, IN. Mr. Ralph James of the Air Force Research Laboratory in Albuquerque, NM was instrumental in authorizing access to the day-to-day cycling data that was collected and stored at the Navy testing facility. Mr. Thomas Miller of the NASA Glenn Research Center in Cleveland, OH was helpful in facilitating access to the NASA-funded cycling database information that was also collected and stored at the Navy facility. The Aerospace Corporation is gratefully acknowledged for supporting this work as part of the Aerospace IR&D program.

Contents

1. Background.....	1
2. Introduction.....	3
3. Earlier Studies.....	5
4. Recent Findings	7
5. Recommendations.....	11
6. Summary	17
References.....	19

Figures

1. Distribution of capacity loss percentages for cells cycled at different temperatures and different DODs.....	3
2. Pressure trend plot for a cell (Cell A) exhibiting a significant amount of capacity walkdown during the first 6,000 charge/discharge cycles.....	4
3. Pressure trend plot from a cell test (Cell B) that was not associated with capacity walkdown.....	4
4. Illustrative Electrochemical Voltage Spectroscopy (EVS) scan of a nickel electrode after the active material has been converted to the more active structure.....	7
5. EVS scans 1 and 2 at +10°C from an electrode taken from Cell B using 26% KOH as the electrolyte. Cycle 2 exhibits the peaks at lower voltages.....	12
6. EVS scans of samples from the same electrode tested at two different temperatures	14

Tables

1. Percentage Capacity Walkdown as a Function of Electrolyte Concentration for Cells Cycled at +10°C.....	11
2. Description of the Electrodes used in the EVS Studies in Reference 3.....	13
3. Summary of Room-Temperature EVS Scans	13
4. Summary of -5°C EVS Scans	13

1. Background

For some mission applications, it is important to maintain the usable capacity of the cell or battery safely above some minimum value. A phenomenon that is associated with nickel-hydrogen cells is known as capacity walkdown. Capacity walkdown is defined as the gradual reduction in the average state-of-charge of a cell during repetitive charge/discharge cycling. When using certain cell designs and cycling conditions, the amount of temporary capacity loss associated with capacity walkdown can typically amount to 35% of the capacity that can be obtained from a fully charged cell. The amount of capacity loss is estimated by the reduction in end-of-charge pressure as monitored by the pressure-measuring device placed on the cell during its manufacture. This walkdown phenomenon was noted during our review¹ of the cycling results generated during NASA- and Air Force-sponsored life-testing studies carried out at the Navy facility located in Crane, IN. Capacity walkdown was found to usually occur during the first 4000 to 8000 cycles following the beginning of a cycling test. It was found to be associated with cells that were being cycled at +10°C and 40% depth-of-discharge (DOD). On the other hand, capacity walkdown was found to be absent from cells being cycled at either -5°C or cycled to 60% DOD.

Earlier studies in our laboratory² into this phenomenon found that capacity walkdown was a result of not fully recharging the capacity that had been discharged during the preceding discharge. Further, this earlier study found that the active material that remained in the discharged state would slowly convert to a slightly different morphological form that had a significantly higher reversible charging potential. The active material became a mixture of two different phases having different reversible charging potentials. For this reason, when an attempt was made to restore this lost capacity, the higher charging voltage that was necessary to charge this modified form of the active material that was now a part of the active material was much closer to the voltage at which significant amounts of oxygen gas were evolved in parallel with charging of the active material. Extra waste heat (reduced charge efficiency) is, therefore, associated with trying to restore the capacity that has walked down. From a reserve capacity standpoint, capacity margin can be lost during the process of capacity walkdown.

More recent studies³ have helped to understand this phenomenon more fully. This newer information documented the changes in the charging voltages for the beta and gamma reactions as impacted by the KOH concentration of the electrolyte, the cobalt content of the active material, and the cycling temperature. The position of these charging peaks, relative to the voltage at which the co-evolution of oxygen at the nickel electrode becomes a significant factor, impacts the charging efficiency of the electrode. This newer data will assist in selecting nickel-hydrogen cell design factors and cycling conditions that will help in the management of the amount of capacity walkdown that takes place. The positions of the charging peaks were found to be a function of the cycling temperature, the KOH concentration of the electrolyte, the cobalt content of the active material, and the cycling history of the electrode. The techniques used in this recent study of the walkdown phenomenon were Electrochemical Voltage Spectroscopy⁴ (EVS) and Flooded Utilization³ (FU). In this recent study, a representative group of electrodes were examined using these electro-analytical techniques. Some elec-

trodes were new, others had been cycled for 40,000 cycles; some had been cycled at +10°C, and others at -5°C; some were cycled in cells using 26% KOH as electrolyte, and others in 31% KOH; and some had a cobalt additive level of about 5%, while others had a cobalt additive level of about 10%. The findings of these studies have resulted in being able to pinpoint the positions of both the charging peaks and discharging peaks associated with the nickel electrode as a function cycling temperature, KOH concentration, cobalt level in the active material, and cycling history of the electrode.

In the studies reported herein, the results of these two previous investigations are focused on understanding and managing the capacity walkdown phenomenon.

2. Introduction

Reserve capacity is that usable capacity that remains in a cell or battery following completion of a normal discharge. If a 100-ampere-hour (Ah) cell is being cycled to 40% DOD, one might expect that there should be 60 Ah of usable capacity following a normal discharge. A review of available cycling data¹ found that this is not the case when cells are cycled to 40% DOD at a temperature of +10°C. On the other hand, when cells are cycled to 60% DOD, this loss is not seen based on end-of-charge (EOC) pressure trends. Likewise, when cells were cycled at -5°C, there was no noticeable capacity loss when cycled at either of these two DODs.

Figure 1 was generated by estimating the capacity loss of cells equipped with strain gauges during the course of their long-term cycling tests. The cells were from the different cell packs that were under test at the Navy facility at Crane, IN. Figure 2 is a typical pressure trend plot from which the loss of end-of-charge pressure could be converted to the number of Ah of lost capacity.

Not all of the cell tests exhibited capacity walkdown as illustrated in Figure 2. Figure 3 is a pressure trend plot that was typical of cell testing that was carried out at -5°C and/or cycled to 60% DOD.

Since capacity walkdown resulted in a temporary loss of usable capacity as well as increased difficulties in restoring the capacity that has walked down, a more in-depth understanding of its cause and possible cure was felt to be important.

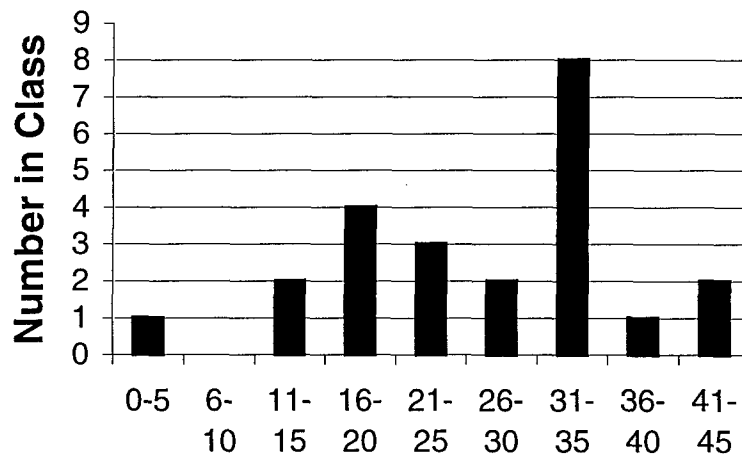


Figure 1. Distribution of capacity loss percentages for cells cycled at different temperatures and different DODs.

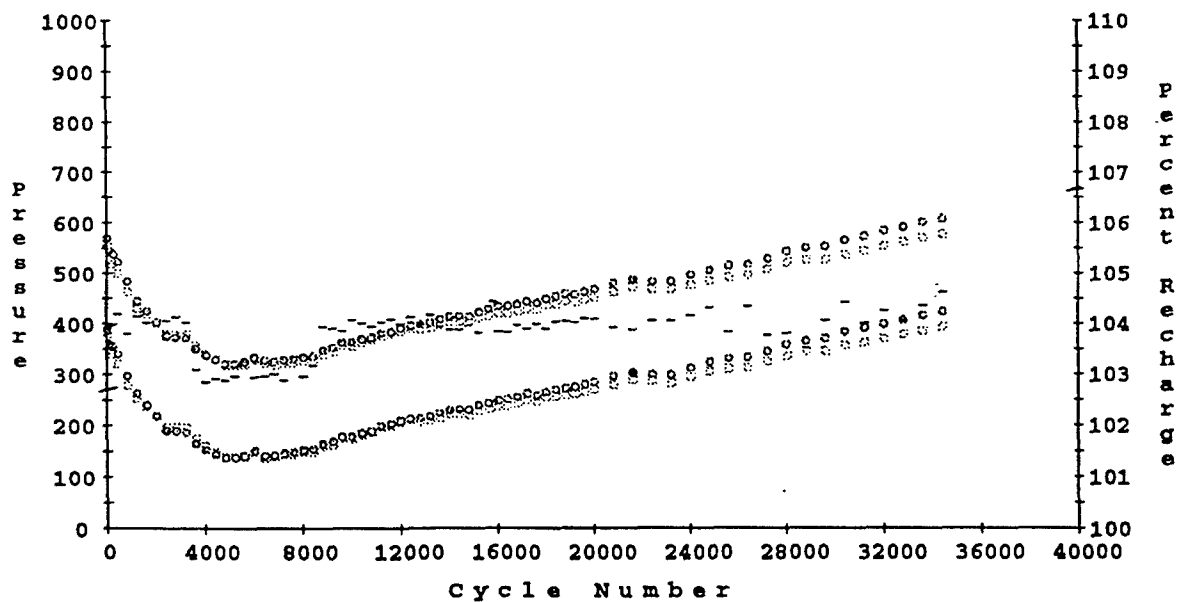


Figure 2. Pressure trend plot for a cell (Cell A) exhibiting a significant amount of capacity walkdown during the first 6,000 charge/discharge cycles.

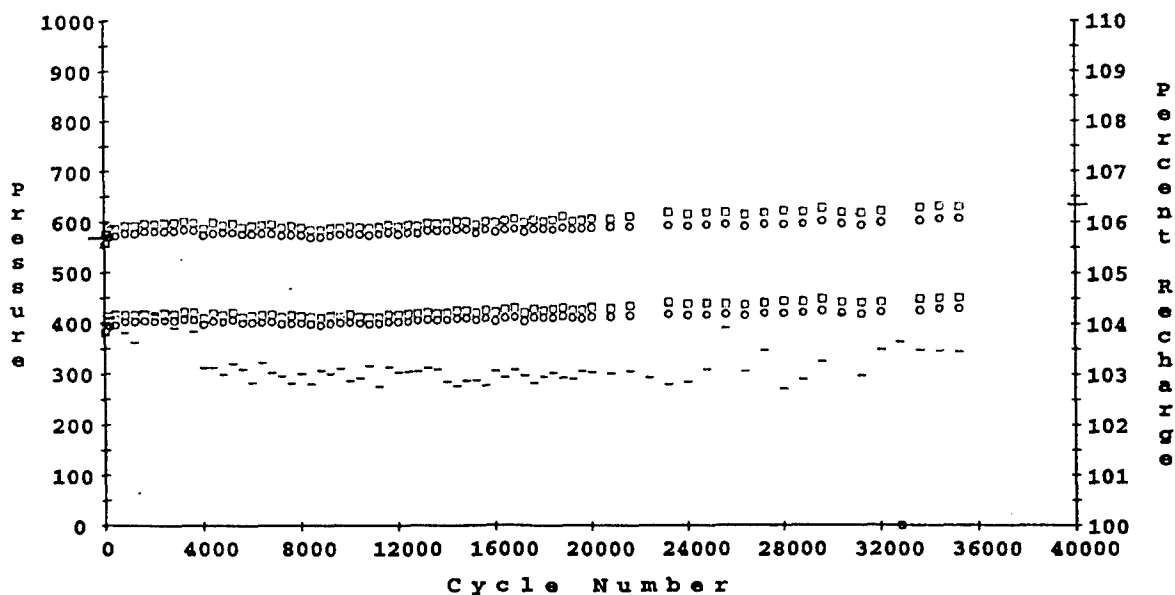


Figure 3. Pressure trend plot from a cell test (Cell B) that was not associated with capacity walkdown.

3. Earlier Studies

During the earlier studies,² several different approaches were taken. First, published pressure and voltage trend plots were reviewed, and amounts of capacity walkdown were estimated using pressure trend information (Figure 1). Since charging protocols were available for these tests, relationships between amounts of capacity loss due to walkdown and charging conditions could be explored. A second approach was to review charging curves of selected cycling tests near to the cycle where the cell reached its minimum in EOC pressure. A third approach was to conduct Electrochemical Voltage Spectroscopy (EVS) studies on selected samples of plate material that had been removed from cells that had experienced different amounts of capacity walkdown. Lastly, several cells that had undergone extensive LEO cycling with significantly different capacity walkdown signatures (Cell A and Cell B) were made available for our further evaluation. The integrated results of these four studies were used to explain reasons for reserve capacity reductions and measures that might be used to reduce it to a minimum or an acceptable amount.

Evidence to date suggests that the temporary loss of usable capacity is caused by a gradual decrease in the charge efficiency of the active material in the nickel electrode as the electrodes were cycled. This can be caused by two different factors. In the first, the oxygen evolution characteristics of the nickel electrode are too close to the potential at which the final portions of the charging process takes place. There is, therefore, a gradual reduction in the state-of-charge of the electrode until equilibrium is reached between these two processes. The second factor involves the gradual buildup of non-cobalt-containing active material adjacent to the nickel substrate due to the slow corrosion of the substrate. Due to the higher reversible potential of this material compared to the cobalt-doped active material,³ there will be a gradual increase in the required charging potential. If constant charging conditions are employed, there will be a gradual drop in the state-of-charge of the active material. Further, it was found that the active material that remained in the discharged state for an extended period of time was converted from an activated form to a deactivated form. These two variants have distinctly different reversible electrode potentials that result in the activated form of the material being oxidized at a potential that is about 40 mV less positive at room temperature than the deactivated form. The gradual buildup of this second phase of active material results in a gradual increase in the charging potential of the nickel electrode. To restore the lost capacity, a higher end-of-charge voltage was needed. Under these conditions, the charge efficiency will be lower. Structural studies to date have not been able to detect a difference in structure of these two materials. Lower cycling temperatures and larger amounts of recharge are conditions that result in lower amounts of capacity walkdown. Of the two, lower cycling temperatures appear to be less stressful on the cell since lower amounts of oxygen evolution are associated with lower cycling temperatures.

4. Recent Findings

This recent study³ has yielded further insight into the phenomenon of capacity walkdown. In this study, the impact of several cell design factors and cycling conditions on the position of the charging peaks for the beta-phase material, the gamma-phase material, and the voltage where oxygen evolution represents a significant parallel reaction during the charging process were quantified. These different potentials were found to change: (1) as the cobalt content of the active material was changed,^{5,6} (2) as the KOH concentration of the electrolyte was changed,^{7,8} and (3) as the cycling temperature was changed.⁹ These findings were in agreement with the referenced studies by other researchers. The potentials at which these reactions occur were also found to change slightly as the electrodes are cycled due to the naturally occurring corrosion processes occurring at the surface of the nickel electrodes. One process is the buildup of the less active form of the active material within the electrode, and the other is the buildup of the non-cobalt-containing corrosion products at the interface next to the nickel sinter. With this newer information, the charge efficiencies as impacted by the cell cycling conditions and the changes caused by the cycling conditions can be more fully understood.

Figure 4 illustrates the relative position of the different charging and discharging peaks of a nickel electrode. The figure is a composite of two different EVS scans. They were generated by very

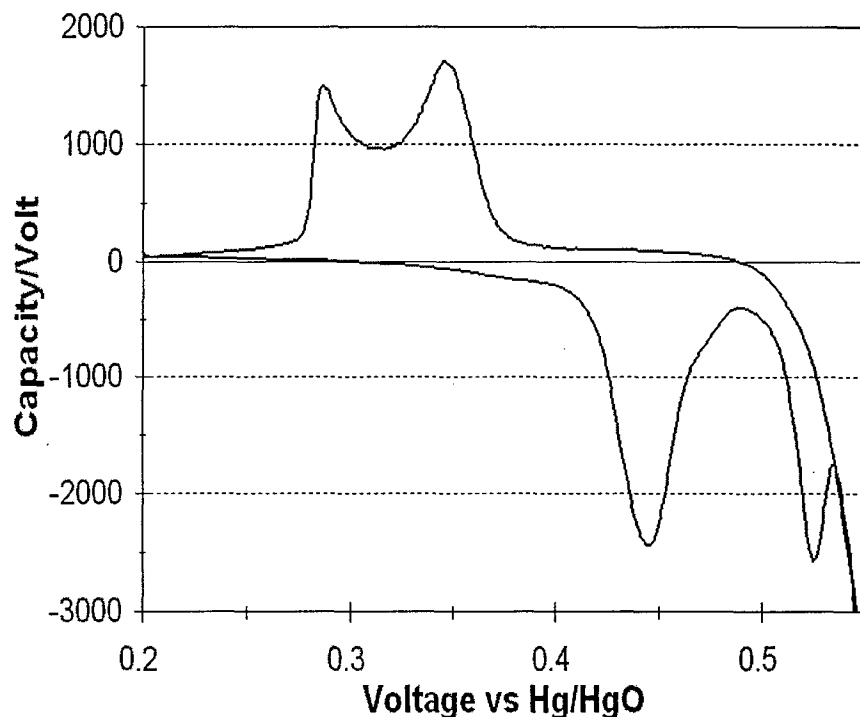


Figure 4. Illustrative Electrochemical Voltage Spectroscopy (EVS) scan of a nickel electrode after the active material has been converted to the more active structure.

slowly charging and discharging a sample of nickel electrode material. The voltage is measured relative to a mercury/mercuric oxide reference electrode. In this plot, the charging part of the scan is shown in the portion below zero, and the discharging portion of the scan appears in the positive portion of the plot. For illustrative purposes, the charging portion of the scan was from one electrode, while the discharge portion of the scan was taken from a different electrode.

Figure 4 may be understood as follows. It is well established that during the charging of nickel electrodes from a fully discharged condition, the active material is first charged to the beta phase as the average valence of the nickel changes from +2 to +3.⁸ Following this, some of the material can be charged to the gamma phase where the average valence of the nickel is +3.66. This second process often occurs in parallel with the evolution of oxygen at the nickel electrode. To increase the usable energy density of the nickel electrode and at the same time to minimize the damage to the electrode and increase the charge efficiency of the charging step, there should be as wide a separation as possible between the potential at which the active material is charged to the gamma phase and the potential at which large amounts of oxygen are evolved. However, at the cycling temperatures in common use, these later two reactions generally occur in parallel at about the same potential.

In the example shown in Figure 4, the broad peak that occurs between about 0.41 V and extending to about 0.49 V is where the discharged active material is charged to the beta form of the active material. The next higher peak, which extends from about 0.50 V to about 0.53 V, is where the charged active material is charged further to the gamma phase. The line to the right of the gamma-charging peak is where the current involved with the formation of oxygen increases logarithmically with potential. During the discharge portion of the cycle, the material that is in the beta phase will discharge first since the voltage at which it discharges is higher than the voltage at which the gamma-phase material discharges. The peaks for these processes occur at about 0.35 V for the discharge of the beta-phase material and 0.27 V for the discharge of the gamma-phase material. The relative amounts of beta- and gamma-material depend on the recharge ratio, end-of-charge voltage, and cycling temperature employed during the charging step. When electrode material is cycled at temperatures and charging rates usually seen in actual cell cycling, the gamma charging peak moves to the right and is often seen only as a shoulder on the oxygen evolution curve.

The exact position of these peaks, especially the charging peaks, is a function of the cobalt content of the active material, the KOH concentration used in the electrolyte, the cycling temperature, and the amount of corrosion that has taken place thus far during the cycling. The charging peaks also depend on whether the active material is in the more active or less active form. These relationships are understood in principle, but the following statements will help quantify them based on our laboratory studies and a review of supporting studies conducted elsewhere.³ By more firmly establishing the location of these peaks as a function of the above-listed variables, issues related to the pros and cons of selecting different cobalt levels, electrolyte KOH concentrations, and cycling temperatures can be examined more accurately.

1. The beta charging peak

The position of this peak is a function of a number of factors. An important one is related to the half-cell potential as impacted by the cobalt content in the active mate-

rial (the higher the cobalt content the lower the half-cell voltage^{5,6}), the KOH concentration (the higher the concentration, the lower the half-cell voltage^{7,8}), the cycling temperature (the higher the temperature, the lower the half-cell voltage⁹), and the relative amounts of more active and less active material.²

2. The gamma charging peak

From extended EVS studies, the gamma peak always appears at a significantly higher voltage than the beta charge peak. Our data suggest that the span between these two peaks at -5°C is between 80 and 90 mV, while at $+25^{\circ}\text{C}$, the span is closer to 50 mV. The position of this peak will move to higher voltages as the electrode is cycled since there will be a buildup of non-cobalt-containing corrosion products adjacent to the nickel sinter current collector. The kinetic factors along with the half-cell voltages combine to establish the shape and the position of this and other peaks as they would appear on an EVS scan.

3. The oxygen evolution reaction

This reaction does not have a peak since the reaction involves the electrolysis of an almost infinite supply of water. Oxygen evolution is an extremely irreversible reaction that thermodynamics would suggest should occur at voltages well below both the theoretical position of the gamma as well as the beta charging peak. There is some evidence that when cobalt is added to the active material, not only do the charging reactions take place at lower voltages, but the oxygen evolution occurs at a slightly higher voltage.⁵ As the temperature is lowered, the kinetics of this highly irreversible reaction are reduced even further, and the voltage at which significant amounts of oxygen are evolved is moved to a higher voltage. At -5°C , the voltage for oxygen evolution occurs about 50 mV higher than at room temperature. This facilitates the separation between the gamma charging peak and prevents the onset of excessive amounts of oxygen evolution. The overall result will be higher charge efficiency, a higher usable energy density when cycling at colder temperatures, and a smaller amount of oxygen evolution. This results in less damage to the nickel electrode during cycling¹⁰ and less waste heat due to the catalytic combination of the evolved oxygen with hydrogen.

4. Activated vs. deactivated potentials

In the case of room temperature EVS studies, this temporary shift is between 20 and 30 mV, while at -5°C , the extent of this shift to higher voltages is between 40 and 60 mV. This shift makes it more difficult to charge electrodes where the active material has been left in the discharged state for an extended period of time. For the case of a 20-cell battery this would require an increase in the end-of-charge voltage of between 0.5 and 1.0 V.

5. Recommendations

The following recommendations will suggest cell design factors and cycling conditions that will result in reduced amounts of capacity loss due to the walkdown phenomenon. Particular attention will be directed towards cells that are filled with 26% KOH vs. those using 31% KOH. Cells filled with 26% KOH have established a solid record of being able to cycle for longer durations than cells filled with 31% KOH.^{11,12} One of the shortcomings identified with cells using 26% KOH as the electrolyte has been their tendency to suffer a greater degree of capacity walkdown compared with cells activated with 31% KOH. Table 1 compares the walkdown results of several side-by-side tests where cells of the same design were cycled after they had been activated with different KOH concentrations.

Larger amounts of capacity walkdown would be expected in cells filled with 26% KOH compared with 31% KOH because the reversible half-cell voltage of the nickel electrode is higher in 26% KOH cell by 10 to 20 mV. This causes more of the charging to take place in parallel with oxygen evolution. The remedy for this is to lower the cycling temperature. This will reduce the amount of oxygen evolution by reducing the kinetics (exchange current) for that reaction. By increasing the cobalt content of the active material, there will be a larger separation between the potential at which the active material is charged and the potential at which oxygen evolution becomes a significant factor.

Table 1. Percentage Capacity Walkdown as a Function of**
Electrolyte Concentration for Cells Cycled at +10°C

Pack Number	Elect. Conc. % KOH	Max. BOL Press.- psi	Walkdown %
1-a	31	606	33
1-b	26	567	42
2-a *	31	605	31
2-b	26	685	20
3-a	31	725	31
3-b	26	680	43
4-a	31	787	14
4-b	26	700	23
5-a	31	795	11
5-b	26	697	35
6-a	31	705	16
6-b	26	660	29

*Based on our newer understanding of the beginning of life capacity as a function of KOH concentration, it is felt that if the information related to tests 2-a and 2-b were reversed in terms of their KOH concentration, it would be more consistent with the other 5 sets of information.

**Estimated from pressure trend data of NASA- and AF-funded cycling test conducted at the Navy facility at Crane, IN.

The impact of KOH concentration and cycling temperature will be illustrated using the EVS scans taken from electrode samples taken from the same plate removed from Cell B. To be noted in Figure 5 is the approximately 40 mV difference between the first and second cycle and the small amount of beta material in the discharge sweeps of both cycles 1 and 2. From our earlier study,² no beta material was seen when charging to a lower voltage of 0.52 V when the electrolyte concentration was 31% KOH. The presence of beta material when charged to a high end-of-charge voltage indicated a smaller amount of capacity in the electrode. The EVS scans taken at -5°C using 31% KOH on samples from the same electrode also showed no evidence of beta material during the discharge portion of the scans.

Tables 2, 3, and 4 from Ref. 3 summarize the information gathered on six different electrodes. Table 2 gives the cycling history of the electrodes selected for this study. Tables 3 and 4 list the peaks for the charging potentials of the beta material, the gamma material, and the potential at which oxygen evolution becomes a significant factor. The peaks are for electrodes that were tested at room temperature (Table 3) and -5°C (Table 4) using 31% KOH as the electrolyte. Some of the electrodes were uncycled whereas others had been cycled for 40,000 cycles. The positions of these peaks were determined using the EVS technique, which generates figures similar to Figure 4.

Based on the position of the gamma charging peak relative to the oxygen evolution character of the nickel electrode, the following generalized statements can be made.

1. Larger amounts of usable capacity are available when cycling is carried out at lower temperatures since the kinetics of the oxygen evolution reaction are reduced, causing the onset of oxygen evolution to occur at higher voltages. This allows a larger percentage of the beta material to be charged to the gamma state prior to the onset of excessive amounts of oxygen evolution. Figure 6 shows this very

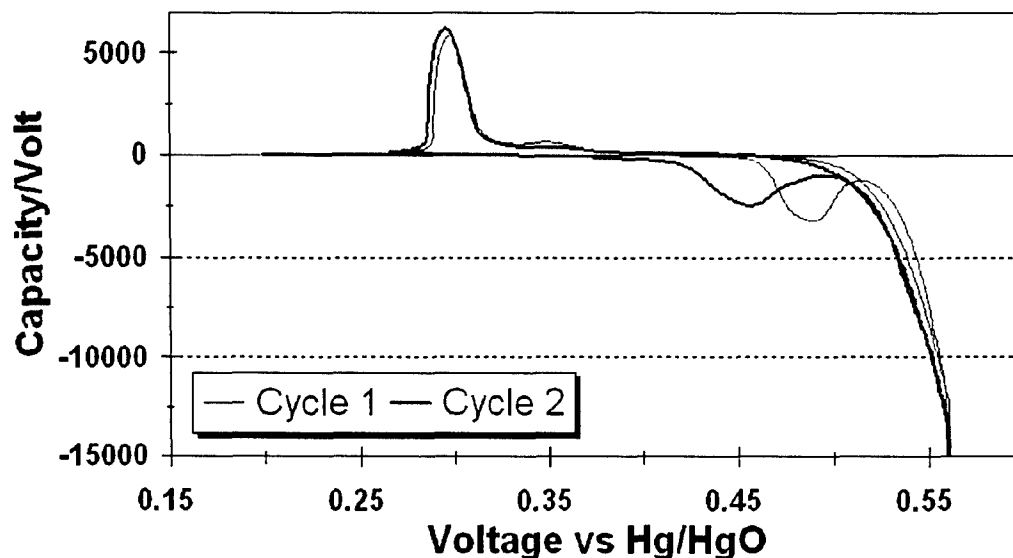


Figure 5. EVS scans 1 and 2 at $+10^{\circ}\text{C}$ from an electrode taken from Cell B using 26% KOH as the electrolyte. Cycle 2 exhibits the peaks at lower voltages.

Table 2. Description of the Electrodes used in the EVS Studies in Reference 3

Plate No.	No. of Cycles	Approx. % Co	Cycling T, °C	Elect. Conc., % KOH	Rech. Ratio, %
1	20	5	+20	31	Varied
2	40,000	5	+10	26	104
3	40,000	5	-5	26	103
4	40,000	10	+10	31	104
5	Not cycled	5	N.A.	N.A.	N.A.
6	Not cycled	10	N.A.	N.A.	N.A.

Table 3. Summary of Room-Temperature EVS Scans

Plate No.	Beta Peak, V	Gamma Peak, V	Oxygen Position, V	Gamma-Beta**, V	Gamma Dis., V
1	0.452	None	0.505	N.A.	0.277
2	0.457	0.51	0.505	0.053	0.277
3	0.450	None	0.505	N.A.	0.276
4	0.456	0.51	0.505	0.054	0.276
5	0.450	None	0.485	0.060	0.272
6	0.408	None	0.505	N.A.	0.262

*The term oxygen position is the voltage at which the rate of oxygen evolution is significant relative to the conversion of active material to the gamma phase. The selected rate of oxygen evolution was equal in all cases.

**The value is the difference in the peak voltages for charging to the beta phase and charging to the gamma phase.

Table 4. Summary of -5°C EVS Scans

Plate No.	Beta Peak, V	Gamma Peak, V	Oxygen Level*, V	Gamma-Beta**, V	Gamma Dis., V
1	0.451	0.532	0.545	0.081	0.278
2	0.450	0.527	0.550	0.077	0.279
3	0.442	0.530	0.550	0.088	0.276
4	0.445	0.525	0.540	0.080	0.278
5	0.442	0.528	0.545	0.086	0.279
6	0.412	None	0.550	N.A.	0.269

*The term oxygen position is the voltage at which the rate of oxygen evolution is significant relative to the conversion of active material to the gamma phase. The selected rate of oxygen evolution was equal in all cases.

**The value is the difference in the peak voltages for charging to the beta phase and charging to the gamma phase.

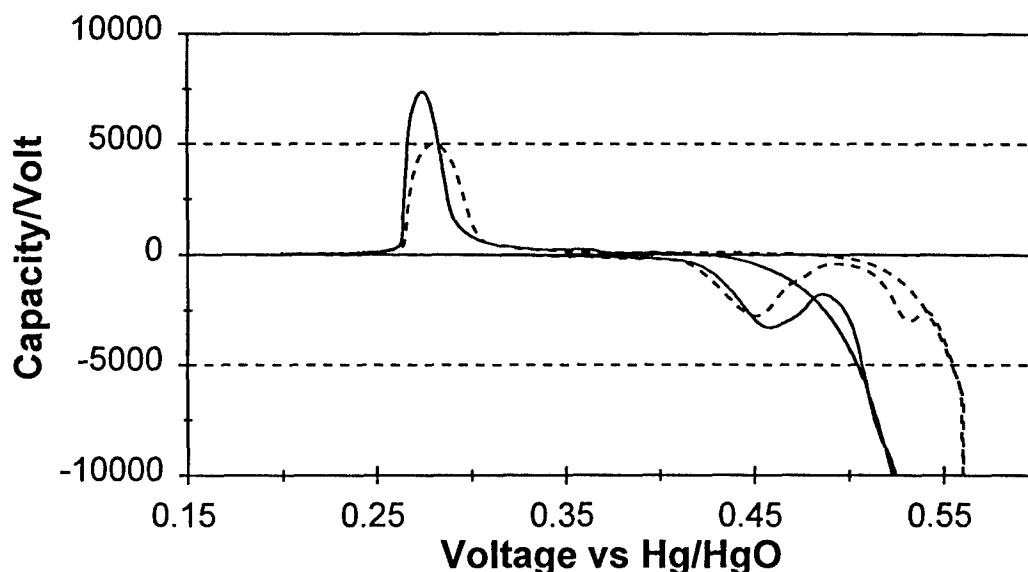


Figure 6. EVS scans of samples from the same electrode tested at two different temperatures. The solid line is cycle 2 at room temperature, and the dotted line is cycle 2 at -5°C . Both tests were carried out in 31% KOH.

clearly. In this figure, the EVS scans for two samples taken from the same electrode are shown. One was scanned at room temperature, and other was scanned at -5°C , both using 31% KOH as electrolyte. The oxygen evolution curve has moved about 50 mV to the right, allowing the charging to the gamma phase of all of the active material prior to the onset of oxygen evolution.

2. Since electrode corrosion occurs over the cycling history of a cell, there is a gradual buildup of non-cobalt-containing active material adjacent to the nickel sinter current collector. A reduction in the cobalt content of the active material increases the voltage needed to charge the electrode. In so doing, there will be a larger amount of oxygen evolved during the charging process. This will result in a gradual reduction in the charging efficiency of the electrode accompanied by a gradual reduction in the state-of-charge of the cell. During long-term cycling, the corrosion process causes the 10% cobalt material to be no different than active material that started out with only 5% cobalt. Both of these electrodes suffer an upward shift in their charging potentials. The remedy for this problem is to lower the cycling temperature. This will reduce the amount of oxygen evolution by reducing the kinetics (exchange current) for that reaction.
3. Increased cobalt content in the active material results in a lower charging voltage for these electrodes. In addition, the reversible potential of the electrodes (as well as the charging peaks) moves further away from the potentials at which oxygen is evolved as cobalt content is increased. This increases the separation between the reactions that result in charging the active material and the reaction resulting in the evolution of oxygen. There is also evidence that the addition of cobalt to the active material increases the

overpotential for oxygen evolution.⁵ By reducing the exchange current of the oxygen evolution reaction, the separation in voltage between the charging reaction and the oxygen evolution reaction is increased even further. As noted in the preceding paragraph, this advantage diminishes with cycling.

4. Active material that is not being charged or discharged will slowly convert to a structural form that changes the voltage at which it is charged or discharged.³ This has been attributed to Ostwald ripening although crystallographic studies have not confirmed these changes. In the case of discharged material at room temperature, a 20 to 30 mV higher voltage must be used to charge this modified form of active material (40 to 60 mV at -5°C). In the case of charged material that has converted to its modified form, a discharge voltage at room temperature that is lower by about 20 mV is experienced during its subsequent discharge. To increase the chargeability of this material, it is suggested that the cycling temperature be reduced to reduce the amount of co-evolution of oxygen gas. When attempting to recharge material that has reverted to the form that is more difficult to recharge, it is important to be able to use an end-of-charge voltage above a threshold value needed to bring about the transition to the form of the active material that charges at a lower voltage.³

6. Summary

The capacity walkdown phenomenon has been revisited following the added information related to the dependence of the charging potential of the gamma-phase material and the oxygen evolution character of the nickel electrode on several cell design factors and the cycling temperature. Cycling conditions and cell design factors must be selected to ensure that the required separation between the charging reactions and the potential at which oxygen evolution becomes a significant factor resulting in a lowering of the charging efficiency. This newer information explains why certain cell design factors (KOH concentration, cobalt level in the active material, and cycling temperature) impact the amount of capacity walkdown during long-term cycling tests. The tendency of cells activated with 26% KOH to walk down further than cells activated with 31% KOH are lessened when cells are cycled at -5°C rather than at $+10^{\circ}\text{C}$. Adjusting the cycling temperature, the KOH concentration, or the cobalt content of the active material can change the amount of walkdown. The gradual buildup of non-cobalt-containing nickel hydroxide corrosion product next to the nickel sinter substrate will result in capacity walkdown as well as selecting inappropriate cycling conditions and cell design factors. The walkdown caused by the buildup of non-cobalt-containing corrosion product is non-recoverable, but is expected to take place over a much longer time span than the walkdown that takes place due to the build up of a mixed phase of active material. This type of walkdown mechanism is recoverable given the proper amount of reconditioning and or overcharge.

References

1. Thaller, L. H., and Zimmerman, A. H., "A Critical Review of Nickel-Hydrogen Life Testing," Aerospace Report No. ATR-2001(8466)-2, May 2001.
2. Thaller, L. H., Zimmerman, A. H., and To, G. A., "Capacity Management and Walkdown During LEO Cycling of Nickel-Hydrogen Cells and Batteries," Aerospace Report No. TR-2001(3310)-1, October 2000.
3. Thaller, L. H., Zimmerman, A. H., and To, G. A., "Techniques to Improve the Usability of Nickel-Hydrogen Cells," Aerospace Report No. ATR- 02(8466)-2, March 2002
4. Thaller, L. H., Zimmerman, A. H., and To, G. A., "Electrochemical Voltage Spectroscopy for Analysis of Nickel Electrodes," Aerospace Report No. TR-2000(8555)-3, January 2000.
5. Armstrong, R. D., Briggs, G. W. D., and Charles, E. A., "Some effects of the addition of cobalt to the nickel hydroxide electrode," *J. of Applies Electrochemistry*, **18**, pp. 215-219, 1988.
6. Watanabe, K., Koseki, M., and Kumagai, N., "Effect of cobalt addition to nickel hydroxide as a positive material for rechargeable alkaline batteries," *J. of Power Sources*, **58**, pp. 23-28, 1996.
7. Dunlop, J. D., Rao, G. M., and Yi, T.Y., *NASA Handbook for Nickel-Hydrogen Batteries*, pp. 5-21, NASA Reference Publication 1314, 1993.
8. Barnard, R., Randell, C. F., and Tye, F. L., "Studies concerning charged nickel hydroxide electrodes. I. Measurement of reversible potentials," *J. of Applies Electrochemistry*, **10**, pp. 109-125, 1980.
9. Faulk, S. U., and Salkind, A. J. *Alkaline Storage Batteries*, p. 533, Wiley and Sons, NY, 1969.
10. Thaller, L. H., "Dealing with Capacity Loss Mechanisms in Nickel-Hydrogen Cells and Batteries," Aerospace Report No. ATR-2001(8466)-4, August 2001.
11. Lim, H. S., and Verzwylt, S. A., "Electrochemical Behavior of Heavily Cycled Nickel Electrodes in Nickel-Hydrogen Cells Containing Electrolytes of Various Concentrations," *Proceedings of the 16th International Power Sources Symposium*, pp. 341-355, Bournemouth, UK, Sept. 1988.
12. Lim, H. S. and Smithrick, J. J., "Advantages of 26% KOH Electrolyte Over Conventional 31% KOH Electrolyte for Nickel-hydrogen Cells," *Proceedings of the 28th IECEC*, **1**, pp. 151-156, Atlanta, GA, Aug. 8-13, 1993.

LABORATORY OPERATIONS

The Aerospace Corporation functions as an "architect-engineer" for national security programs, specializing in advanced military space systems. The Corporation's Laboratory Operations supports the effective and timely development and operation of national security systems through scientific research and the application of advanced technology. Vital to the success of the Corporation is the technical staff's wide-ranging expertise and its ability to stay abreast of new technological developments and program support issues associated with rapidly evolving space systems. Contributing capabilities are provided by these individual organizations:

Electronics and Photonics Laboratory: Microelectronics, VLSI reliability, failure analysis, solid-state device physics, compound semiconductors, radiation effects, infrared and CCD detector devices, data storage and display technologies; lasers and electro-optics, solid state laser design, micro-optics, optical communications, and fiber optic sensors; atomic frequency standards, applied laser spectroscopy, laser chemistry, atmospheric propagation and beam control, LIDAR/LADAR remote sensing; solar cell and array testing and evaluation, battery electrochemistry, battery testing and evaluation.

Space Materials Laboratory: Evaluation and characterizations of new materials and processing techniques: metals, alloys, ceramics, polymers, thin films, and composites; development of advanced deposition processes; nondestructive evaluation, component failure analysis and reliability; structural mechanics, fracture mechanics, and stress corrosion; analysis and evaluation of materials at cryogenic and elevated temperatures; launch vehicle fluid mechanics, heat transfer and flight dynamics; aerothermodynamics; chemical and electric propulsion; environmental chemistry; combustion processes; space environment effects on materials, hardening and vulnerability assessment; contamination, thermal and structural control; lubrication and surface phenomena.

Space Science Applications Laboratory: Magnetospheric, auroral and cosmic ray physics, wave-particle interactions, magnetospheric plasma waves; atmospheric and ionospheric physics, density and composition of the upper atmosphere, remote sensing using atmospheric radiation; solar physics, infrared astronomy, infrared signature analysis; infrared surveillance, imaging, remote sensing, and hyperspectral imaging; effects of solar activity, magnetic storms and nuclear explosions on the Earth's atmosphere, ionosphere and magnetosphere; effects of electromagnetic and particulate radiations on space systems; space instrumentation, design fabrication and test; environmental chemistry, trace detection; atmospheric chemical reactions, atmospheric optics, light scattering, state-specific chemical reactions and radiative signatures of missile plumes.

Center for Microtechnology: Microelectromechanical systems (MEMS) for space applications; assessment of microtechnology space applications; laser micromachining; laser-surface physical and chemical interactions; micropropulsion; micro- and nanosatellite mission analysis; intelligent microinstruments for monitoring space and launch system environments.

Office of Spectral Applications: Multispectral and hyperspectral sensor development; data analysis and algorithm development; applications of multispectral and hyperspectral imagery to defense, civil space, commercial, and environmental missions.